The Journal of Chemical Physics

RESEARCH ARTICLE | MAY 06 2025

On the origin of the breakloose friction force

Special Collection: Festschrift for Abraham Nitzan

T. Tada ; B. N. J. Persson

Check for updates

J. Chem. Phys. 162, 174709 (2025)
https://doi.org/10.1063/5.0266065

View Online
Export Citation

Articles You May Be Interested In

Comparison by computer fluid dynamics of the drag force acting upon two helmets for wheelchair racers

AIP Conf. Proc. (July 2017)

Modeling swimsuits

Physics Today (August 2008)

Model of the 2003 Tour de France

Am. J. Phys. (May 2004)

11 August 2025 05:24:07

Webinar From Noise to Knowledge

May 13th – Register now

Zurich Instruments
Universität Konstanz

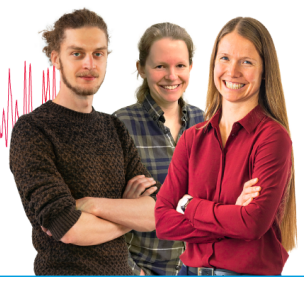

AIP Publishing

The Journal of Chemical Physics ARTICLE pubs.aip.org/aip/jcp

On the origin of the breakloose friction force

Cite as: J. Chem. Phys. 162, 174709 (2025); doi: 10.1063/5.0266065
Submitted: 17 February 2025 • Accepted: 28 March 2025 •
Published Online: 6 May 2025

View Online Export Citation CrossMark

T. Tada[1] and B. N. J. Persson[2,3,4,a)]

AFFILIATIONS

[1] Sumitomo Rubber Industries, Research and Development, HQ. 2-1-1, Tsutsui-cho, Chuo-ku, Kobe 651-0071, Japan
[2] Peter Grünberg Institute (PGI-1), Forschungszentrum Jülich, 52425 Jülich, Germany
[3] State Key Laboratory of Solid Lubrication, Lanzhou Institute of Chemical Physics, Chinese Academy of Sciences, 730000 Lanzhou, China
[4] MultiscaleConsulting, Wolfshovener Str. 2, 52428 Jülich, Germany

Note: This paper is part of the JCP Special Topic, Festschrift for Abraham Nitzan.
[a)] **Author to whom correspondence should be addressed:** b.persson@fz-juelich.de

ABSTRACT

We discuss the origin of the static or breakloose friction force and describe a *kinetic effect* that can manifest itself as an (effective) breakloose friction force. The kinetic effect is important if the kinetic friction force $F_k(v)$ has a maximum at low sliding speed, say for $v = v_c$. If the driving speed v is higher than v_c, the friction force at the onset of slip will first increase rapidly to approximately $F_k(v_c)$ and then rapidly decrease to $F_k(v)$, resulting in an effective breakloose friction force larger than the kinetic friction force. We present experimental results for sliding friction of a racer rubber tread compound and a passenger car tread compound, which exhibit very different breakloose friction as a result of this kinetic effect. We show that pre-slip in the contact makes the breakloose friction be less than the product of the true contact area and static shear stress. For elastically soft materials, in the absence of the kinetic effect described above, this may result in a breakloose friction force equal to the kinetic friction force. We present experimental results for a passenger car tread compound, which illustrate this effect.

© 2025 Author(s). All article content, except where otherwise noted, is licensed under a Creative Commons Attribution (CC BY) license (https://creativecommons.org/licenses/by/4.0/). https://doi.org/10.1063/5.0266065

11 August 2025 05:24:07

INTRODUCTION

The area of real contact when two elastic solids with random roughness are squeezed together by a normal force F_N is typically proportional to the normal force.[1–9] This proportionality holds even when adhesion increases the contact area, assuming that the adhesion does not manifest itself as a pull-off force—a condition satisfied in most practical applications, e.g., negligible adhesion when lifting a bottle from a table.[10] When the real contact area remains proportional to F_N, the sliding friction force is generally also proportional to F_N. In such cases, one defines static and kinetic friction coefficients (μ_s and μ_k), where the force required to initiate sliding (breakloose friction force) equals $\mu_s F_N$, while the friction force during steady sliding equals $\mu_k F_N$.

Most physics textbooks introduce the concepts of static and kinetic friction coefficients without detailed explanation. The kinetic friction force is defined as the friction force acting on an object (denoted as a block in the following discussion) during steady sliding. However, the static friction force depends on multiple factors, including stationary contact duration, sliding history, and how the external force is applied to the block. Some of these aspects were recognized already by friction research pioneers such as C. A. Coulomb, as described in the book of Dowson.[11]

In this Letter, we discuss the origin of static (breakloose) friction forces[12–18] and identify a kinetic effect critically important in rubber friction. We present experimental results for sliding friction using a racer tread compound and a passenger car tread compound, which demonstrate significantly different breakloose friction behavior due to this kinetic effect.

BREAKLOOSE FRICTION FORCE

The breakloose friction force (also called static friction force) depends on the history of contact between two solids. For example, the longer one waits in stationary contact, the larger the breakloose friction force may become due to either a slow increase in the

© Author(s) 2025

contact area or thermally activated (and hence contact time-dependent) bond formation at the interface. Other processes that can lower the interfacial free energy and increase the break-loose friction force, could result from plasticity and viscoelasticity in the confining walls or structural relaxation of the boundary lubricant.

The breakloose friction also depends on sliding history prior to stationary contact.[19,20] For instance, if a block slides on a substrate, the resulting temperature increase in the block, particularly near asperity contact regions, may affect the friction force. If the block motion stops, the temperature distribution in the block (and substrate asperity contact regions) evolves over time, resulting in a breakloose friction force that depends on the contact duration. This effect is particularly significant for rubber materials, where rapid flash temperature changes can cause substantial friction variations during non-stationary sliding.

Memory effects in sliding friction are often taken into account using state variables governed by phenomenological equations of motion,[21–23] an approach widely adopted in earthquake dynamics studies.

The breakloose friction force is the maximum in the friction force before steady sliding and is usually denoted as the static friction force. However, we do not like the latter notation since most people associate it with a well-defined quantity (many tables of static friction coefficients exist), which is not the case since it depends on the history of the contact, which is usually not. Here, we define the *maximum static friction force*, F_s, as the product of the (static) frictional shear stress times the contact area. This would be the force needed to start sliding (again dependent on the history of the contact) if the solids would be rigid, so all contact regions would break at the same time.

Strengthening of a contact during stationary contact does not always produce a breakloose friction force exceeding the kinetic friction force, in particular for elastically soft materials. We now analyze this phenomenon with a specific focus on rubber friction.

Consider a "kinetic" frictional shear stress τ_k acting on contact area A between a block and a substrate during sliding. For simplicity, we assume τ_k to be velocity-independent (in practice, this is almost never the case, and for rubber friction, the variation with sliding speed can be very large). After a stationary contact duration t_s, the shear stress at the new onset of sliding (sliding initiation) becomes τ_s, which we assume is larger than τ_k, e.g., due to thermally activated interfacial bond formation. For this case, the breakloose friction force F_B is fundamentally dependent on material compliance and is governed by two length scales:

The first length scale λ_{asp} represents the sliding distance required to break asperity contacts (and form new contacts), which is comparable to their linear dimensions. Actual systems exhibit asperity size distributions,[24–27] with shear stress changes occurring at nanometer displacements. Complete contact renewal requires displacements comparable to the largest asperity contact regions (0.1–1 mm for rubber–road interfaces, typically 1–10 μm for other materials). The second length scale λ_{el} depends on material elasticity, nominal contact pressure distribution, and tangential force application method. For example, if a rectangular elastic block (height h and length in the sliding direction $L >> h$) is loaded with a force on one side as in Fig. 1(a), we have $\lambda_{el} \approx (\tau_s - \tau_k)L^2/Eh$, where E is the Young's modulus (see below).

Figure 1 shows the slip initiation during the sliding onset for three cases. Because of the elasticity of the solid, the slip area (black regions in Fig. 1) continuously expands until global sliding occurs across the entire surface. [The case (b) in Fig. 1 is the famous Cattaneo–Mindlin case, which can be studied analytically with some simplifying assumptions; see Refs. 28–31]. Assuming that $u(\mathbf{x}, t)$ is the elastic deformation-induced slip at the interface before global sliding, we have the following:

- Rigid solids show $u = 0$ at the onset (initiation) of slip and exhibit simultaneous motion at all interface points
- Deformable solids show increased u with decreasing elastic modulus, due to the delayed motion propagation from the force application point

In regions where $u > \lambda_{asp}$, the contact is (locally) renewed; thus, the frictional shear stress is equal to the kinetic shear stress τ_k. Consequently,

- Rigid solids require displacement $u > \lambda_{asp}$ to reach F_k, maintaining $F_B = A\tau_s > A\tau_k = F_k$ during the onset of sliding ($u = 0$), i.e., the breakloose friction force equals the maximum static friction force.

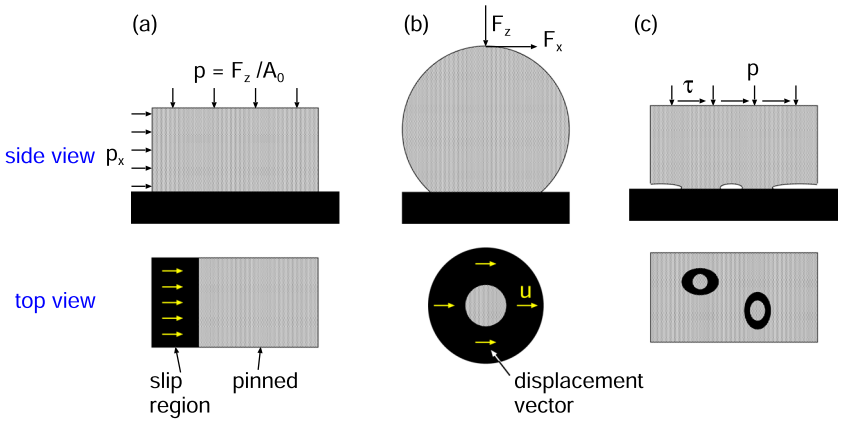

FIG. 1. Slip at the onset of sliding in three different cases [(a)–(c)]. There is a continuous increase in the area where slip occurs as the system approaches the onset of global slip, where the full contact area is slipping. The frictional shear stress in the region where the slip $u > \lambda_{asp}$ is equal to the kinetic frictional shear stress τ_k. Consequently, the breakloose friction force will be smaller than $F_s = A\tau_s$ and will approach $F_k = A\tau_k$ as the elastic modulus decreases.

11 August 2025 05:24:07

© Author(s) 2025

- $F_B < A\tau_s$ for deformable solids, approaching $F_k = A\tau_k$ with decreasing elastic modulus.

The second length scale is non-zero only for deformable solids, as demonstrated in three examples (a)–(c).

In Fig. 1(a), slip initiates at the tangential force application point, whereas in (b) and (c), it begins at contact region boundaries where contact pressure minimizes. For case (a), we define the dimensionless parameter

$$\alpha = \frac{\lambda_{el}}{\lambda_{asp}} \approx \frac{(\tau_s - \tau_k)L^2}{Eh\lambda_{asp}}, \tag{1}$$

where L is the block length in the slip direction, h is the block height, and E is the elastic modulus of the block (substrate assumed rigid). As shown in Ref. 13, $F_B \approx A\tau_s$ when $\alpha \ll 1$, while $F_B \approx F_k$ when $\alpha \gg 1$.

α is the relevant parameter for determining the magnitude of the breakloose friction force which can be understood from the following qualitative argument. At the onset of full slip, the stress at the interface between the block and the substrate ranges between τ_k and τ_s, corresponding to a force between $\tau_k Lw$ and $\tau_s Lw$, where w is the width of the block perpendicular to the sliding direction. This equals to the backside force $F_x = p_x hw$, where pressure $p_x = \tau L/h$ $(\tau_k < \tau < \tau_s)$. Part of this pressure compresses the block in the sliding direction, creating average displacement u determined by $\Delta p \approx E\epsilon$, with strain $\epsilon = u/L$. This gives $u \approx L\Delta p/E$, and assuming $\Delta p \approx (\tau_s - \tau_k)L/h$, we obtain $u \approx (\tau_s - \tau_k)L^2/(Eh)$. If $u \ll \lambda_{asp}$, we expect the breakloose friction force to be $F_B \approx A\tau_s$, while if $u \gg \lambda_{asp}$, we expect $F_B \approx A\tau_k$. Since $\alpha = u/\lambda_{asp}$, this yields the condition described above.

The influence of elasticity on breakloose force decreases with system size. This follows from (1): maintaining constant L/h (so the shape of the block remains similar) while reducing the linear size gives $\alpha \sim L$. Thus, for sufficiently small L, we have $\alpha \ll 1$ and $F_B = \tau_s A$, explaining why small objects exhibit larger breakloose than kinetic friction, as observed experimentally.[14] This is analogous to the dependence of adhesion on the pull-off force as the system size decreases. In larger systems, bond breaking between two solids usually occurs via interfacial crack propagation, whereas in very small and elastically stiff solids, the bonds break more uniformly at the interface during normal pull-off.[32,33]

In general, at the onset of global slip, the surface displacement $u(\mathbf{x})$ is non-uniform, either due to how the external force is applied [case (a)] or due to non-uniform nominal normal contact stress, as in cases (b) and (c). If the slip $u > \lambda_{asp}$ over most of the contact area at the onset of global slip, one expects $F_B \approx F_k$, but this is not always the case due to the following *kinetic* effect.

Figure 2(a) shows the friction coefficient as a function of the sliding speed acting on an elastic block, where we assume that the $\mu_k(v)$ curve has a maximum at $v = v_c$, with $\mu_k(v_c) = \mu_c$. If the block is stationary for $t < 0$ and the upper surface of the block moves with velocity v for $t > 0$, the friction force F_x acting on the block will rapidly (and monotonically) increase to $\mu_k(v)F_N$ if $v < v_c$ [case (b)], whereas if $v > v_c$, the friction force will first increase rapidly to approximately $\mu_c F_N$ and then decrease rapidly to $F_k = \mu_k(v_b)F_N$ [case (c)]. For a rigid block, these changes in the friction force would occur instantaneously (with negligible block displacement),

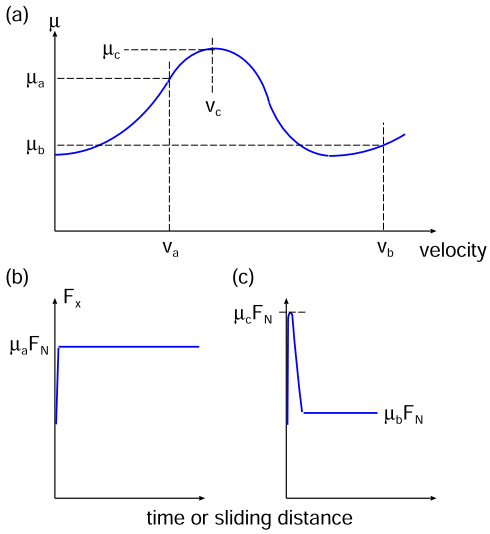

FIG. 2. (a) Friction coefficient as a function of sliding speed. The $\mu_k(v)$ curve exhibits a maximum at $v = v_c$, where $\mu_k(v_c) = \mu_c$. If a rubber block is stationary for $t < 0$ and the upper surface of the block moves with velocity v for $t > 0$, the friction force F_x acting on the block will rapidly (and monotonically) increase to $\mu_k(v)F_N$ if $v < v_c$ [case (b)]. However, if $v > v_c$, the friction force will first increase rapidly to approximately $\mu_c F_N$ and then rapidly decrease to $F_k = \mu_k(v_b)F_N$ [case (c)].

but for a block with finite elasticity, the change would occur continuously. However, the transition happens so rapidly that the peak force appears as a breakloose (or static) friction force. In the first case, the effective static or breakloose friction force equals the kinetic friction force, while in the second case, it equals approximately $\mu_c F_N$.

Note that the breakloose friction equals exactly $\mu_c F_N$ only if the slip velocity at the interface is uniform when the average velocity reaches v_c. This is not always the case, as different surface regions may begin to slip at different times. In particular, if v_c is very small, some parts of the interface may move faster than v_c when the average interface speed equals v_c. In this case, the effective breakloose friction force will be less than $\mu_c F_N$ but still greater than the kinetic friction force F_k.

EXPERIMENTAL RESULTS

We illustrate the discussion above with experimental results for two types of rubber sliding on concrete surfaces.

For rubber friction on rough surfaces at room temperature, the friction force typically reaches a maximum at a sliding speed of ~10 mm s^{-1} for passenger car tires, whereas for racing tires, this maximum occurs at much lower speeds, around 1 μm/s. The key reason for this difference is that racing tires are designed to operate at much higher temperatures—typically around 100 °C or more—compared to passenger car tires, where the operating temperature is typically around 60 °C. Since the peak in the friction coefficient shifts with temperature according to the bulk viscoelastic shift factor a_T, the friction coefficient maximum in both cases may occur at sliding speeds on the order of a few meters per second when the tires are used at their optimal (design) temperature.

11 August 2025 05:24:07

© Author(s) 2025

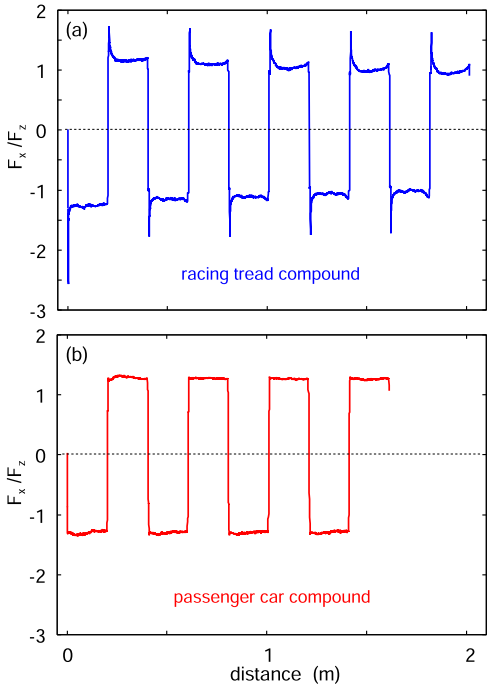

FIG. 3. Ratio between the tangential (friction) force F_x and the normal force F_N = 250 N as a function of the sliding distance during oscillatory movement of rubber blocks for a racing compound (a) and a passenger car compound (b), sliding on concrete surfaces at T = 20 °C. The rubber blocks first move forward at v = 3 mm s^{-1} for 20 cm and then backward at the same velocity, returning to the starting point. This motion is repeated five times for the racing compound and four times for the passenger car compound. The rubber blocks are 0.5 cm high with lateral dimensions of 4 × 4 cm^2.

This difference in frictional properties between passenger car and racing tires is achieved by using rubber compounds with very different glass transition temperatures (T_g), typically ranging from −40 to −60 °C for passenger car tires and approximately −15 °C or higher for racing tires. [For the compounds in Fig. 3, T_g = −12 °C (racing compound) and −44 °C (passenger car compound); see the Appendix.] A lower T_g (at a fixed temperature) results in greater polymer chain mobility, meaning a higher sliding speed is required for the pulsating rubber–road asperity contacts to reach the viscoelastic transition region, where viscoelastic energy dissipation—and thus friction force—is maximized.

The experimental results were obtained using a linear reciprocal friction slider, as described in detail elsewhere.[34] The setup consists of a rubber block ($A_0 \approx 16$ cm^2) glued onto an aluminum plate sample holder, which is connected to a force cell. The rubber specimen moves vertically with the carriage to adapt to the substrate profile. The normal load is adjustable by adding additional steel weights on top of the force cell.

The substrate (a concrete block) is fixed to the machine table, which moves transversely using a servo drive via a gearbox. This setup allows precise control of the relative velocity between the rubber specimen and the substrate, while the force cell records the normal and frictional forces.

Figure 3(a) shows the ratio of the tangential (friction) force F_x to the normal force F_N at T = 20 °C as a function of the sliding distance for a racing compound with T_g = −12 °C. The rubber block first moves forward at v = 3 mm s^{-1} for 20 cm then reverses direction at the same velocity, returning to the starting point. This motion is repeated five times.

Notably, large friction peaks appear when the velocity changes sign, where the bottom surface of the rubber block undergoes an abrupt (yet continuous) velocity reversal from v = 3 to −3 mm s^{-1}. This is expected since friction studies show that the racing compound exhibits a maximum friction at $v \approx 1$ μm/s.

When the peak in the friction coefficient occurs above the sliding speed v, we do not expect a friction peak upon velocity reversal. To illustrate this case, Fig. 3(b) presents the friction force for a rubber block of a passenger car tire (with a glass transition temperature T_g = −50 °C). In this case, no friction peak is observed during velocity reversal. In addition, the breakloose friction force is equal to the kinetic friction force, i.e., $F_B = F_k$. This is due to the low elastic modulus of the rubber: at the onset of global slip, most of the contact area has moved sufficiently to reduce the frictional shear stress from τ_s to τ_k.

For the racing compound, the breakloose friction force is larger than the peak in the friction force observed during velocity reversal. This may be attributed to a larger real contact area at the initiation of sliding compared to that during velocity reversal, where the system spends a very short time near $v \approx 0$. An increase in the contact area depending on the stationary contact duration is also expected for the passenger car compound. However, this effect is not evident in the friction force curve in Fig. 3(b) for the following reason:

For the passenger car rubber compound, the frictional shear stress increases with sliding speed. When the velocity reaches the driving speed of 3 mm s^{-1}, the bottom surface of the block has already slipped a sufficient distance to renew the asperity contact regions, reaching the steady-state sliding contact area. At this sliding speed, the flash temperature effect is negligible, and the rubber temperature remains constant.

SUMMARY AND CONCLUSION

We have discussed the origin of the static or breakloose friction force, with a focus on a kinetic effect that plays a crucial role in friction dynamics, particularly in rubber friction, such as in tires or the breakloose friction force of rubber stoppers in syringes. If the friction force as a function of sliding speed exhibits a maximum at velocities much lower than those of practical interest, this maximum can result in an effective breakloose friction force and a peak in the friction force whenever the sliding velocity changes sign.

This effect is particularly relevant for tire dynamics simulations and can, in some cases, simplify such simulations if v_c is sufficiently small, so that slip at velocities below v_c can be neglected. For example, when a tire operates at small slip, the tread blocks initially deform elastically with negligible slip until the force reaches the friction maximum (at $v = v_c$), after which rapid slip occurs.[35,36] In this case, the maximum of $\mu_k(v)$ effectively acts as a static friction coefficient, determining the boundary in the tire–road footprint that separates tread blocks experiencing negligible slip from those undergoing rapid sliding.

11 August 2025 05:24:07

© Author(s) 2025

ACKNOWLEDGMENTS

Bo Persson acknowledges many years of scientific collaboration and friendship with Abraham Nitzan (Abe). We first met at the beautiful *Vibration at Surfaces* conference in Asilomar, California, in 1982. At that time, Abe was interested in surface enhanced Raman scattering, a topic that also interested me, and we had a long discussion. He contributed to this field with fundamental work on the enhancement of the electromagnetic field in the vicinity of particles or surface inhomogeneities. After that, I visited him many times at Tel Aviv University, and he also visited me at FZ-Jülich. Abe is an inspiring and hard-working scientist. During one of his visits to FZ-Jülich, we worked on a model for vibrational dephasing at surfaces. One morning, when I arrived at work, Abe was already there—it turned out he had worked through the entire night. It is my sincere hope that Abe remains in good health and continues contributing to science for many more years.

AUTHOR DECLARATIONS

Conflict of Interest

The authors have no conflicts to disclose.

Author Contributions

T. Tada and B.N.J. Persson have contributed equally to all aspects of this work.

T. Tada: Conceptualization (equal); Data curation (equal); Formal analysis (equal); Funding acquisition (equal); Investigation (equal); Methodology (equal); Project administration (equal); Resources (equal); Software (equal); Supervision (equal); Validation (equal); Visualization (equal); Writing – original draft (equal); Writing – review & editing (equal). **B. N. J. Persson**: Conceptualization (equal); Data curation (equal); Formal analysis (equal); Funding acquisition (equal); Investigation (equal); Methodology (equal); Project administration (equal); Resources (equal); Software (equal); Supervision (equal); Validation (equal); Visualization (equal); Writing – original draft (equal); Writing – review & editing (equal).

DATA AVAILABILITY

The data that support the findings of this study are available within the article.

APPENDIX: VISCOELASTIC MODULUS AND RUBBER FRICTION MASTER CURVES

We have measured the viscoelastic modulus of the racing and passenger car compounds in elongation mode for the strain amplitude 4×10^{-4} (or 0.04% strain).[37] At this small strain, we probe the linear response properties of the rubber. Figure 4 shows the temperature dependence of the modulus for the frequency $\omega_0 = 0.01\ s^{-1}$. We define the glass transition temperature as the temperature where ImE/ReE is maximal, which gives $T_g = -44$ and $-12\,^{\circ}C$ for the passenger car and racing tire compounds, respectively. We have found in the past that using the reference frequency $\omega_0 = 0.01\ s^{-1}$ when defining T_g gives glass transition temperatures close to what is obtained from standard thermodynamic methods.

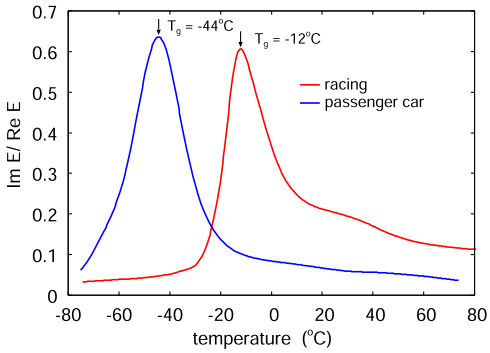

FIG. 4. Temperature dependency of ImE/Re E for the frequency $\omega = 0.011$/s. The viscoelastic modulus $E(\omega, T)$ was measured at a very low strain, so the stress is proportional to the strain (linear response).

The friction results were obtained using the low-temperature linear friction described elsewhere.[38] With this setup, we can change the temperature from −40 to 20 °C and the sliding speed from 1 μm/s to 1 cm s^{-1}. All measurements were performed on concrete surfaces of the same type as used in earlier studies. The rubber surfaces were cleaned with warm water and soft brush. During run-in, a thin rubber surface layer is removed. After the sliding act reported in Fig. 3, the surfaces of both the racer compound and the passenger car compound appear relatively smooth, i.e., no big damaged areas occur on the surfaces. This is consistent with Fig. 3, which shows that the forward–backward sliding cycles result in nearly the same time-dependent friction force for the first sliding cycle as for the last cycle. The concrete substrate has much higher roughness than the rubber surfaces, and we believe that this is much more important for

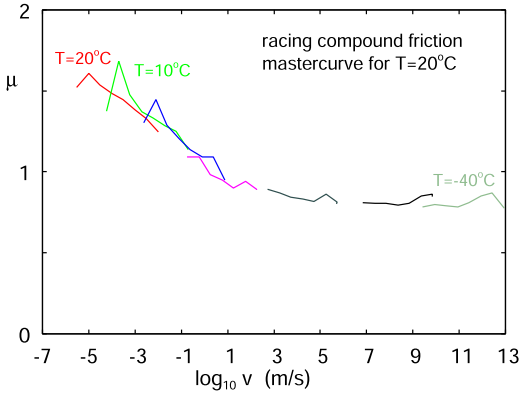

FIG. 5. Sliding friction master curve for the racing compound. The friction velocity segments were measured for temperatures between −40 and 20 °C and shifted along the velocity axis using the viscoelastic shift factor a_T obtained when calculating the viscoelastic master curve $E(\omega, T_0)$. The reference temperature is $T_0 = 20\,^{\circ}C$.

11 August 2025 05:24:07

© Author(s) 2025

the friction force than the (sliding induced) roughness on the rubber surfaces. Some contamination (darken sliding track) of the concrete surfaces can be observed after the sliding acts shown in Fig. 3 and may be the reason for the slight reduction in the friction force for the racer compound between the first and the last sliding cycle (each sliding cycle is over the same concrete surface area).

From measurements performed at different temperatures and for the velocity interval from 3 μm/s to 1 cm s^{-1}, we can construct friction master curves. For passenger car tires, the master curves at room temperature have maximum typically in the range from 0.1 to 10 cm s^{-1}, but for racing compounds, the maximum occurs at much lower sliding speeds for the reason discussed in the text.

Figure 5 shows the sliding friction master curve for the racing compound. The friction velocity segments were measured for temperatures between −40 and 20 °C and shifted along the velocity axis using the viscoelastic shift factor a_T obtained when calculating the viscoelastic master curve $E(\omega, T_0)$. The reference temperature $T_0 = 20$ °C. The master curve has a maximum below the lowest measured sliding speed 3 μm/s. Using the bulk shift factor a_T, the master curve shifts to higher speeds with ≈6 velocity decades at $T = 85$ °C and by ≈7 velocity decades at $T = 105$ °C, resulting in a maximum in the friction in the velocity range (1–10 m/s) of most interest for racing.

REFERENCES

[1] B. N. J. Persson, "Theory of rubber friction and contact mechanics," J. Chem. Phys. **115**, 3840 (2001).

[2] S. Hyun, L. Pei, J. F. Molinari, and M. O. Robbins, "Finite element analysis of contact between elastic self affine surfaces," Phys. Rev. E **70**, 026117 (2004).

[3] N. Prodanov, W. B. Dapp, and M. H. Müser, "On the contact area and mean gap of rough, elastic contacts: Dimensional analysis, numerical corrections, and reference data," Tribol. Lett. **53**, 433 (2014).

[4] C. Yang and B. N. J. Persson, "Contact mechanics: Contact area and interfacial separation from small contact to full contact," J. Phys.: Condens. Matter **20**, 215214 (2008).

[5] B. N. J. Persson, "Contact mechanics for randomly rough surfaces," Surf. Sci. Rep. **61**, 201 (2006).

[6] H. Terwisscha-Dekker, A. M. Brouwer, B. Weber, and D. Bonn, "Elastic contact between rough surfaces: Bridging the gap between theory and experiment," J. Mech. Phys. Solids **188**, 105676 (2024).

[7] F. Kaiser, D. Savio, and R. Bactavatchalou, "Modelling of static and dynamic elastomer friction in dry conditions," Lubricants **12**, 250 (2024).

[8] M. H. Müser, "How static is static friction?," Proc. Natl. Acad. Sci. U. S. A. **105**, 13187 (2008).

[9] S. Sills *et al.*, "Molecular origins of elastomeric friction," in *Nanotribology: Friction and Wear on the Atomic Scale*, edited by E. Gnecco and E. Meyer (Springer Verlag, 2007), Chap. 30, pp. 659–676.

[10] B. N. J. Persson, I. M. Sivebaek, V. N. Samoilov, K. Zhao, A. I. Volokitin, and Z. Zhang, "On the origin of Amonton's friction law," J. Phys.: Condens. Matter **20**, 395006 (2008).

[11] D. Dowson, *History of Tribology* (Longman, New York, 1979).

[12] B. N. J. Persson, O. Albohr, F. Mancosu, V. Peveri, V. N. Samoilov, and I. M. Sivebaek, "On the nature of the static friction, kinetic friction and creep," Wear **254**, 835 (2003).

[13] B. Lorenz and B. N. J. Persson, "On the origin of why static or breakloose friction is larger than kinetic friction, and how to reduce it: The role of aging, elasticity and sequential interfacial slip," J. Phys.: Condens. Matter **24**, 225008 (2012).

[14] L. Peng, T. Roch, D. Bonn, and B. Weber, "Why static friction decreases from single to multi-asperity contacts," Phys. Rev. Lett. **134**, 176202 (2024).

[15] G. He, M. H. Muser, and M. O. Robbins, "Adsorbed layers and the origin of static friction," Science **284**, 1650 (1999).

[16] M. H. Müser, L. Wenning, and M. O. Robbins, "Simple microscopic theory of Amontons's laws for static friction," Phys. Rev. Lett. **86**, 1295 (2001).

[17] M. H. Müser, M. Urbakh, and M. O. Robbins, "Statistical mechanics of static and low-velocity kinetic friction," Adv. Chem. Phys. **126**, 187 (2003).

[18] A. Papangelo, M. Ciavarella, and J. R. Barber, "Fracture mechanics implications for apparent static friction coefficient in contact problems involving slip-weakening laws," Proc. R. Soc. A **471**, 20150271 (2015).

[19] O. M. Braun, I. Barel, and M. Urbakh, "Dynamics of transition from static to kinetic friction," Phys. Rev. Lett. **103**, 194301 (2009).

[20] R. Capozza and M. Urbakh, "Static friction and the dynamics of interfacial rupture," Phys. Rev. B **86**, 085430 (2012).

[21] J. H. Dieterich, "Modeling of rock friction: 1. Experimental results and constitutive equations," J. Geophys. Res. **84**, 2161, https://doi.org/10.1029/jb084ib05p02161 (1979).

[22] A. Ruina, "Slip instability and state variable friction laws," J. Geophys. Res.: Solid Earth **88**, 10359, https://doi.org/10.1029/jb088ib12p10359 (1983).

[23] B. N. J. Persson, *Sliding Friction: Physical Principles and Applications*, 2nd ed. (Springer, 2000).

[24] J. H. Dieterich, and B. D. Kilgove, "Direct observation of frictional contacts: New insight for state-dependent properties," Pure Appl. Geophys. **143**, 283 (1944).

[25] M. H. Müser and A. Wang, "Contact-patch-size distribution and limits of self-affinity in contacts between randomly rough surfaces," Lubricants **6**, 85 (2018).

[26] C. Campañá, M. H. Müser, and M. O. Robbins, "Elastic contact between self-affine surfaces: Comparison of numerical stress and contact correlation functions with analytic predictions," J. Phys.: Condens. Matter **20**, 354013 (2008).

[27] B. N. J. Persson, R. Xu, and N. Miyashita, "Rubber wear: Experiment and theory," J. Chem. Phys. **162**, 074704 (2025).

[28] C. Cattaneo, *Sul Contato di Due Corpo Elastici*, *Rendiconti, Series 6* (Accademia dei Lincei, 1938), Vol. 27, pp. 342–348, 434–436, and 474–478.

[29] R. D. Mindlin, "Compliance of elastic bodies in contact," J. Appl. Mech. **16**, 259 (1949).

[30] I. Etsion, "Revisiting the Cattaneo–Mindlin concept of interfacial slip in tangentially loaded compliant bodies," J. Tribol. **132**, 020801 (2010).

[31] M. Ciavarella, "Transition from stick to slip in Hertzian contact with 'Griffith' friction: The Cattaneo–Mindlin problem revisited," J. Mech. Phys. Solids **84**, 313 (2015).

[32] B. N. J. Persson, "Nanoadhesion," Wear **254**, 832 (2003).

[33] M. H. Müser and B. N. J. Persson, "Crack and pull-off dynamics of adhesive, viscoelastic solids," Europhys. Lett. **137**, 36004 (2022).

[34] A. Tiwari, N. Miyashita, N. Espallargas, and B. N. J. Persson, "Rubber friction: The contribution from the area of real contact," J. Chem. Phys. **148**, 224701 (2018).

[35] B. N. J. Persson, "Rubber friction and tire dynamics," J. Phys.: Condens. Matter **23**, 015003 (2011).

[36] M. Selig, B. Lorenz, D. Henrichmöller, K. Schmidt, A. Ball, and B. Persson, "Rubber friction and tire dynamics: A comparison of theory with experimental data," Tire Sci. Technol. **42**, 216 (2014).

[37] B. Lorenz, W. Pyckhout-Hintzen, and B. N. J. Persson, "Master curve of viscoelastic solid: Using causality to determine the optimal shifting procedure, and to test the accuracy of measured data," Polymer **55**, 565 (2014).

[38] A. Tiwari, N. Miyashita, and B. N. J. Persson, "Rolling friction of elastomers: Role of strain softening," Soft Matter **15**, 9233 (2019).

11 August 2025 05:24:07

© Author(s) 2025